

AC-field-controlled localization-delocalization transition in one dimensional disordered system

Wei Zhang and Sergio E. Ulloa

Department of Physics and Astronomy, and Nanoscale and Quantum Phenomena Institute, Ohio University, Athens, OH 45701-2979

(Dated: September 4, 2018)

Based on the random dimer model, we study correlated disorder in a one dimensional system driven by a strong AC field. As the correlations in a random system may generate extended states and enhance transport in DC fields, we explore the role that AC fields have on these properties. We find that similar to ordered structures, AC fields renormalize the effective hopping constant to a smaller value, and thus help to localize a state. We find that AC fields control then a localization-delocalization transition in a given one dimensional systems with correlated disorder. The competition between band renormalization (band collapse/dynamic localization), Anderson localization, and the structure correlation is shown to result in interesting transport properties.

PACS numbers: 72.15.Rn,72.10.Bg,73.21.-b

Keywords: correlations, disorder, AC field, dynamical localization

I. INTRODUCTION

The dynamics of electrons in ordered semiconductor superlattices driven by electric fields has received a great deal of attention. For example, well-known predictions for quantum mechanical behavior, such as Wannier-Stark ladders and Bloch oscillations, which are difficult to observe in ordinary solids, were verified in beautiful experiments.¹ Furthermore, behavior such as negative differential conductance,² fractional Wannier-Stark ladders,³ excitonic Franz-Keldysh effect,⁴ among others, have been the focus of recent work. Of particular recent interest are the localization and delocalization behavior of electrons in the presence of external electric fields, which have direct effect on the macroscopic transport properties of the system. For example, in a system with both AC and DC fields, an appropriate AC field will delocalize the Wannier-Stark ladder states induced by a strong pure DC field.⁵ An intense AC field can by itself also lead to *dynamical localization* of the carriers.⁶ This phenomenon has been studied extensively in various systems,⁷ especially in quantum dot pairs,⁸ and finite linear arrays.⁹

Certainly, disorder or imperfections are unavoidable in a real system. It is widely known that localization due to disorder plays a fundamental role in a variety of physical situations. In particular, it has been of interest to investigate disordered systems in the presence of electric fields: Hone *et al.*,¹⁰ and Zhang *et al.*¹¹ studied the case of one impurity in the presence of AC fields. Holthaus *et al.* studied AC-field-controlled Anderson localization in disordered semiconductor superlattices.¹² As scaling theory shows that all eigenstates in disordered one-dimensional (1D) systems are localized,¹³ previous studies have focused on the effects of electric fields on the localization length.¹²

On a related area, the existence of metallic states in a class of conducting polymers, such as polyaniline and heavily doped polyacetylene, was identified by Dunlap

*et al.*¹⁴ with *extended states* in 1D systems that exist if short-range correlations in the disordered structure are taken into account. The existence of extended states in this *random dimer model* was also verified in experiments with GaAs-AlGaAs superlattices designed to exhibit such correlated disorder.¹⁵

More general correlations have also been studied in 1D systems. Perturbation theories for the random dimer model were developed in Ref. [16], and particle transport in models with correlated diagonal and off-diagonal disorder were discussed also by Flores.¹⁷ The random dimer model driven by a DC field was studied in¹⁸. The delocalization behavior in 1D models with long-ranged correlated disorder for the on-site energies was studied by a renormalization technique,¹⁹ and by a Hamiltonian approach.²⁰ More recently, the Kronig-Penney model with correlated disorder was studied,²¹ demonstrating that a mobility edge may exist for disordered systems with appropriate long-range correlated disorder. The role of structural correlations in the sequence disorder in DNA molecules has also been studied recently,^{22,23} as this represents a real system that exhibits structural correlations between the diagonal and off-diagonal elements in a tight-binding representation.

In this rich context, it is important to study the competition between dynamic localization (due to AC field), Anderson localization (due to disorder) and the correlation in the disorder, and to investigate the role of external fields on the transition from the localized to the delocalized state in 1D systems. In this paper, we concentrate on the short range correlations of the random dimer model, and study the localization-delocalization transition driven by external AC electric fields. We find that AC electric fields induce a transition from extended to localized states under suitable conditions, and find the transition point analytically in the high frequency limit. We also show that the transition for lower frequencies is shifted in field, as a precursor of DC-field results. Although our results are for a relatively simple 1D model

potential, we expect that they will be relevant for a variety of dissimilar systems, including polymers,¹⁴ exciton transfer in active media,²⁴ semiconductor superlattices,¹⁵ quantum dot arrays,⁹ and even hole transport in complex molecules^{22,23}, as their dynamics is described well by effective 1D models.

After introducing our general model in Sec. II and presenting an analysis of the high frequency regime for the

single-dimer system in Sec. III, we present numerical results and general discussions in Sec. IV.

II. RANDOM DIMER MODEL IN AC ELECTRIC FIELDS

A. Model

We consider a 1D random dimer model driven by an AC electric field. The appropriate Hamiltonian is then

$$H = \sum_m \{ \varepsilon_m a_m^+ a_m + R(a_{m+1}^+ a_m + a_m a_{m+1}^+) + medE(t) a_m^+ a_m \}, \quad (1)$$

where R is the hopping amplitude between nearest neighbors, $E(t) = E_1 \cos(\omega t)$ is the time-dependent field with frequency ω , d is the constant separation between chain sites, and the on-site energy parameter is $\varepsilon_m = \varepsilon_a$ (or ε_b) with probability Q (or $1 - Q$; here we typically choose $Q = 1/2$, as it represents the most disordered system, although other values are also used), and ε_b is assigned to a pair of nearest neighbor sites when it occurs. Since the Hamiltonian is periodic in time, the Floquet theorem implies that the state can be written as

$$\psi(x, t) = e^{-i\varepsilon t} \sum_n C_n(t) \phi_n(x), \quad (2)$$

where ε is the quasi-energy, ϕ_n is the Wannier state and C_n is the probability amplitude for an electron on site n at time t , which is periodic in time, i.e., $C_n(t) = C_n(t + T)$, with $T = 2\pi/\omega$. The Schrödinger equation

$$i \frac{\partial}{\partial t} \psi(x, t) = H \psi(x, t) \quad (3)$$

can then be written as

$$i \frac{\partial}{\partial t} C_n(t) = (\varepsilon_n - \varepsilon) C_n(t) + R(C_{n+1} + C_{n-1}) + nedE_1 \cos(\omega t) C_n. \quad (4)$$

Since the term containing the electric field is proportional to n , it is not suitable to perform perturbative calculations. We introduce the following transformation

$$C'_n(t) = C_n(t) e^{i n \beta \sin(\omega t)}, \quad (5)$$

where $\beta = edE_1/\omega$. It is easy to see that $|C'_n(t)| = |C_n(t)|$, $C'_n(t + T) = C'_n(t)$, and that $C'_n(t)$ satisfies the equation

$$i \frac{\partial}{\partial t} C'_n(t) = (\varepsilon_n - \varepsilon) C'_n(t) + R(e^{-i\beta \sin(\omega t)} C'_{n+1} + e^{i\beta \sin(\omega t)} C'_{n-1}). \quad (6)$$

Since $C'_n(t)$ is periodic in time, we can expand it in Fourier series, $C'_n(t) = \sum_m A_n^m e^{im\omega t}$. Using the identity²⁵

$$e^{iz \sin(\theta)} = \sum_{m=-\infty}^{+\infty} (-1)^m J_m(z) e^{-im\theta}, \quad (7)$$

where J_m is the m -th Bessel function, we can obtain an equation for A_n^m

$$(\varepsilon_n - \varepsilon + m\omega) A_n^m + R \sum_l [A_{n+1}^{m+l} (-1)^l J_l(-\beta) + A_{n-1}^{m+l} (-1)^l J_l(\beta)] = 0. \quad (8)$$

B. High frequency limit

We analyze here the behavior of our model in the high frequency regime. Apart from illustrative, this limit is of practical importance, since much interest exists in systems driven by THz fields.^{4,26} In the high frequency limit, A_n^0 gives the most important contribution to $C_n(t)$. The equation for A_n^0 is

$$(\varepsilon_n - \varepsilon) A_n^0 + R \sum_l (A_{n+1}^l (-1)^l J_l(-\beta) + A_{n-1}^l (-1)^l J_l(\beta)) = 0. \quad (9)$$

We first keep only the terms with $l = 0$, and obtain,

$$(\varepsilon_n - \varepsilon)A_n^0 = RJ_0(\beta)(A_{n+1}^0 + A_{n-1}^0). \quad (10)$$

This equation indicates simply that in the high frequency limit, the effect of the AC field is to suppress hopping and change R to an effective hopping constant $R_{\text{eff}} = RJ_0(\beta)$. This is a well-known result in driven systems.⁷

Let us consider the corrections coming from terms containing $A_n^{\pm 1}$. The relevant equations are

$$(\varepsilon_n - \varepsilon)A_n^0 + RJ_0(\beta)(A_{n+1}^0 + A_{n-1}^0) + RJ_1(\beta)(A_{n+1}^1 - A_{n+1}^{-1} - A_{n-1}^1 + A_{n-1}^{-1}) = 0$$

$$(\varepsilon_n - \varepsilon + \omega)A_n^1 + RJ_0(\beta)(A_{n+1}^1 + A_{n-1}^1) - RJ_1(\beta)(A_{n+1}^0 - A_{n-1}^0) = 0$$

and

$$(\varepsilon_n - \varepsilon - \omega)A_n^{-1} + RJ_0(\beta)(A_{n+1}^{-1} + A_{n-1}^{-1}) + RJ_1(\beta)(A_{n+1}^0 - A_{n-1}^0) = 0. \quad (11)$$

These equations (11) can be further simplified, and in conjunction with (10), we find that

$$\begin{aligned} (B_{n+1} - B_{n-1}) \left(1 - \left(\frac{RJ_0}{\omega} \right)^2 \right) &= \frac{2R^2 J_0 J_1}{\omega^2} (A_{n+1}^0 + A_{n-1}^0) \\ &+ \left(\frac{RJ_0}{\omega} \right)^2 (B_{n+3} - B_{n-3}) - \frac{2R^2 J_0 J_1}{\omega^2} (A_{n+3}^0 + A_{n-3}^0), \end{aligned} \quad (12)$$

where we have defined $B_n = A_n^1 - A_n^{-1}$. Thus the higher Fourier component corrections to the effective bandwidth $R_{\text{eff}} = RJ_0(\beta)$ are of higher order in R/ω , which of course makes them small in the high frequency limit, $R/\omega \ll 1$. In this limit, the model with AC field behaves essentially as a system *without* electric field, except for a rescaling of the bandwidth given to the lowest order by $R_{\text{eff}} = RJ_0 \left(\frac{edE_1}{\omega} \right)$.

In the random dimer model without AC field, the localization-delocalization transition occurs when $\varepsilon_- = |\varepsilon_a - \varepsilon_b|$ is twice the bandwidth.¹⁴ We then intuitively expect that $\varepsilon_- = 2R_{\text{eff}}$ would be the transition point between localized and delocalized states in the presence of the AC field. Before giving numerical evidence for this transition in the full random dimer system, we analyze the single impurity case to gain further understanding of this problem.

III. SINGLE IMPURITY-DIMER CASE

It is instructive to see what happens when only one impurity-dimer is involved in an otherwise periodic 1D chain. We consider both the cases with and without an AC field for comparison.

A. Static case

Let us first consider the scattering effects introduced by a single *site*-impurity in a chain, in the absence of AC field.¹⁴ We let all site energies be ε_a , except for site 0

where it is ε_b . From the eigenvalue equation

$$(\varepsilon_n - \varepsilon)C_n + R(C_{n+1} + C_{n-1}) = 0, \quad (13)$$

we can get the transmission probability

$$|T|^2 = \frac{(4R \sin kd)^2}{\varepsilon_-^2 + (4R \sin kd)^2}, \quad (14)$$

where k is the wave vector of the incoming Bloch wave, and $\varepsilon_- = |\varepsilon_b - \varepsilon_a|$ measures the impurity *detuning*, and as such is a measure of the “disorder” or impurity strength. One can see that for this one-impurity case, $|T|^2 < 1$ for $\varepsilon_- \neq 0$. In a random multi-impurity system, a series of n scattering events would naturally lead to $|T|^{2n} \ll 1$, and very small amplitude for the outgoing wave, resulting in localization in the thermodynamic limit.

If instead, we assign a pair of sites 0 and 1 with energy ε_b to form a single dimer impurity, the transmission probability is¹⁴

$$|T|^2 = 1 - \frac{\varepsilon_-^2 (\varepsilon_- + 2R \cos kd)^2}{\varepsilon_-^2 (\varepsilon_- + 2R \cos kd)^2 + 4R^2 \sin^2 kd}. \quad (15)$$

In this *one impurity-dimer* case, $|T| = 1$, whenever $\varepsilon_- = -2R \cos kd$. This is a sort of resonance effect due to the internal structure of the impurities. Thus, in the presence of the peculiar kind of short-range correlated disorder described by the random dimer model, there are states with unity transmission probability, which clearly have an extended character (even if they only appear at a single value of the energy). This one impurity-dimer calculation, makes intuitive the appearance of extended states in the random multi-dimer system at peculiar energy values, and captures qualitatively the reason for the unusual behavior of the random dimer model [14,27].

B. The case with AC electric field

We now turn to explore what happens when an AC electric field is turned on. Hone *et al.* studied the system of an isolated defect driven by strong electric fields.¹⁰ We will make use of Green's functions in terms the Floquet formalism. We consider the resolvent operator as a function of the complex frequency z

$$G(z) = \frac{1}{z - H} = G^0(z) + G^0(z)VG(z), \quad (16)$$

where $H = H_0 + V$, H_0 is the unperturbed Hamiltonian, V is the impurity potential, and $G^0(z) = \frac{1}{z - H_0}$. In the representation of Wannier states, the Green's function is

$$G_{jl} = G_{jl}^0 + \sum G_{jj'}^0 V_{j'l'} G_{l'l}. \quad (17)$$

In the high frequency limit, $R/\omega \ll 1$, G^0 is¹⁰

$$G_{jl}^0 = \frac{1}{R_{\text{eff}}} \frac{q^{|l-j|+1}}{1 - q^2}, \quad (18)$$

where $R_{\text{eff}} = R J_0 \left(\frac{edE_1}{\omega} \right)$, and

$$q = \frac{\tilde{z}}{2R_{\text{eff}}} \pm \sqrt{\frac{\tilde{z}^2}{4R_{\text{eff}}^2} - 1}. \quad (19)$$

The sign is chosen such that q falls inside the unit circle. For an isolated defect with $V_{jl} = \nu \delta_{j,0} \delta_{0,l}$ (where $\nu = \varepsilon_- = |\varepsilon_b - \varepsilon_a|$ is the case of different site energy), the probability $p(l)$ for the defect state (with energy $\varepsilon = R_{\text{eff}}(q + \frac{1}{q})$) to occupy the l^{th} site is determined by the residue of G_{ll} . One finds that¹⁰

$$p(l) = \frac{\nu}{\sqrt{\nu^2 + 4R_{\text{eff}}^2}} \left(\sqrt{\frac{\nu^2}{4R_{\text{eff}}^2} + 1} - \left| \frac{\nu}{2R_{\text{eff}}} \right| \right)^{2|l|}. \quad (20)$$

Notice that $p(l)$ falls exponentially from the site $l = 0$ where the defect is localized, with a characteristic decay length that is reduced for increasing $|\nu|/R_{\text{eff}}$, as one might suspect.

Now we consider a one-dimer model, with $V_{jl} = \nu(\delta_{j,0}\delta_{0,l} + \delta_{j,1}\delta_{1,l})$, and $\nu = \varepsilon_-$. After some calculation, we find

$$\begin{aligned} G_{ll} &= G_{ll}^0 + \nu G_{l0}^0 G_{0l} + \nu G_{l1}^0 G_{1l} \\ G_{0l} &= \frac{\nu G_{10}^0 G_{1l}^0 + (1 - \nu G_{00}^0) G_{0l}^0}{(1 - \nu G_{00}^0)(1 - \nu G_{11}^0) - \nu^2 G_{10}^0 G_{01}^0} \\ G_{1l} &= \frac{\nu G_{10}^0 G_{0l}^0 + (1 - \nu G_{00}^0) G_{1l}^0}{(1 - \nu G_{00}^0)(1 - \nu G_{11}^0) - \nu^2 G_{10}^0 G_{01}^0}, \end{aligned} \quad (21)$$

so that

$$G_{ll} = aq + \frac{1}{2} \nu a^2 q^{2l} \left[\frac{(1+q)^2}{1 - aq(1+q)} - \frac{(1-q)^2}{1 - aq(1-q)} \right], \quad (22)$$

where a is defined as $\frac{\nu}{R_{\text{eff}}(1 - q^2)}$. Defining $\gamma = \frac{\nu}{2R_{\text{eff}}}$, for the pole at $q_1 = \frac{1}{2\gamma + 1}$, we get

$$p(l) \sim (q_1)^{2l}, \quad (23)$$

and since $q_1 < 1$, this corresponds to a localized state. For the pole $q_2 = \frac{1}{2\gamma - 1}$, one gets

$$p(l) \sim (q_2)^{2l}. \quad (24)$$

When $\nu = \varepsilon_- > 2R_{\text{eff}}$, $q_2 < 1$, and this corresponds to a localized state with localization length $\sim 1/\ln(2\gamma - 1)$. When γ approaches 1 from above, the localization length diverges, indicating a transition to a delocalized state. Thus the single dimer impurity in an AC field yields the same conclusion as in the high frequency case, and the transition from localized to extended states occurs at the point $\nu = 2R_{\text{eff}}$.

IV. NUMERICAL RESULTS AND DISCUSSION

Most of our numerical calculations were performed on a chain with 1501 sites. We solved equation (4) with initial condition $C_n(t = 0) = \delta_{n,0}$, and analyze the subsequent development. The site energies were chosen from a bi-valued distribution, $\varepsilon_n = \varepsilon_a$ and $\varepsilon_n = \varepsilon_b$, with probability $\frac{1}{2}$. As the site prob remains, the “degree of disorder” is controlled by larger values of $\varepsilon_- = |\varepsilon_b - \varepsilon_a|$, as we will see in what follows.

A. High frequency regime $\frac{R}{\omega} \ll 1$

In Fig. 1 we show numerical calculations of the mean-square displacement, $\langle m^2 \rangle = \sum_n n^2 |C_n|^2$, versus time. One can see in curve (a) that when $\varepsilon_- = |\varepsilon_b - \varepsilon_a| = R_{\text{eff}}$, the mean-square displacement $\langle m^2 \rangle \sim t^{3/2}$. This is known as the *superdiffusive transport* regime. Diffusive transport ($\langle m^2 \rangle \sim t$) is shown either when $\varepsilon_- = 0.97 \cdot 2R_{\text{eff}}$ (curve b) or perhaps for $\varepsilon_- = 2R_{\text{eff}}$ (curve c). On the other hand, curve (d) for $\varepsilon_- = 2R = 2.27R_{\text{eff}}$ shows how the mean square displacement is increasingly bounded (subdiffusive), $\langle m^2 \rangle \sim t^{0.36}$. Further increasing $\varepsilon_- > 2R_{\text{eff}}$, as shown in curve (e) ($\varepsilon_- = \omega = 3.78R_{\text{eff}}$) results in completely bounded motion $\langle m^2 \rangle \approx \text{const.}$, as anticipated from the analytical discussion above. We believe the subdiffusive behavior for $\varepsilon_- = 2R > 2R_{\text{eff}}$ is a crossover behavior due to finite size effects, masking the anticipated extended \rightarrow localization transition at $\varepsilon_- = 2R_{\text{eff}}$. In fact, from the Eq. (15) (with R replaced by R_{eff}) for the transmission probability, we may estimate the localization length $\lambda \sim -1/\ln|T(k)|^2 \sim \frac{1}{\delta + \beta k^2}$, where $\varepsilon_- = -\delta - 2R_{\text{eff}}$, and δ is small. The number of “extended states” (states with localization length λ larger than the system size L) is $\Delta N \sim L(\frac{1}{L} - \delta)^{1/2}$.

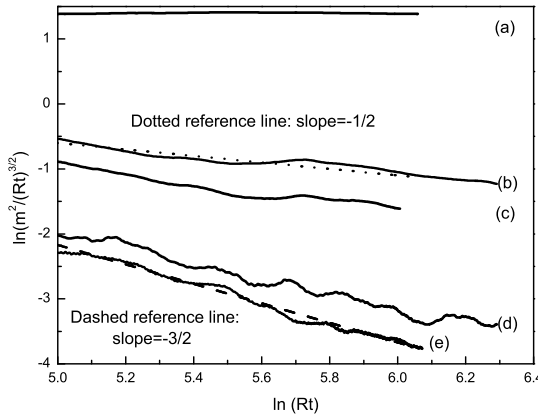


FIG. 1: The mean-square displacement divided by $(Rt)^{3/2}$ for varying amounts of disorder in the high frequency regime $R/\omega = 0.3$. Amplitude of AC electric field is $\beta = edE_1/\omega = 0.7$; effective hopping constant $R_{\text{eff}} = R J_0(\beta) = 0.8812R$. (a) With $\varepsilon_- = |\varepsilon_b - \varepsilon_a| = R_{\text{eff}}$ results in superdiffusive transport, $\langle m^2 \rangle \sim t^{3/2}$; while (b) $\varepsilon_- = 0.97 \cdot 2R_{\text{eff}}$, and (c) $\varepsilon_- = 2R_{\text{eff}}$ result in diffusive behavior, $\langle m^2 \rangle \sim t$, compared with dotted line of slope $-1/2$. For (d) $\varepsilon_- = 2R$, we see $\langle m^2 \rangle$ is nearly bounded, and for (e) $\varepsilon_- = \omega = 3.78R_{\text{eff}}$, we find completely bounded $\langle m^2 \rangle$, compared with dashed slope $-3/2$.

We believe these “extended states” lead to the subdiffusive behavior. With increasing of δ , as in curve (e), or increasing system size, one gets $\Delta N = 0$, if $\frac{1}{N} < \delta$. It is very difficult to go beyond the crossover regime by numerical simulations, as it requires simulations in very large system sizes, with longer equilibration times, requiring longer simulation time to obtain accurate values of the self-averaged quantities in a $\ln Rt$ fashion. Scaling studies of this transition would be interesting.

The structure of Fig. 1 is similar to that shown in [14] in the absence of AC fields. For a fixed AC electric field amplitude, there is a transition from extended to localized state behavior with increasing disorder. The role of AC electric fields can be seen to effectively decrease the hopping constant, thus contributing to the localization of carriers. For example, for $\varepsilon_- \leq 2R$, in the case *without* electric fields, results in extended states (and diffusive transport).¹⁴ However, when an AC electric field (with $edE_1/\omega = 0.7$) is turned on, the mean squared displacement is suppressed. This localization-delocalization transition is clearly induced by the AC electric field, as the transition shifts to $\varepsilon \simeq 2R_{\text{eff}}$.

It is interesting to see the situation for a stronger field $\beta = edE_1/\omega = 2.405$, (the first root of J_0). In this case, $R_{\text{eff}} = 0$, and we expect that even for very weak disorder the state will be localized. Our results in Fig. 2 (with very small disorder, $\varepsilon_-/R = 0.33$) show that this is indeed the case. This is also in agreement with the fact

that even in the limit of $\varepsilon_- = 0$, i.e. when there is no disorder, the states are localized when band collapse occurs (i.e. $R_{\text{eff}} = 0$).²⁸ This is nothing but the well-known dynamical localization.⁶ In Fig. 2 one notices that there are oscillations in the mean square displacement. This is the manifestation of the time dependence of the electric field in this case of weak disorder. In fact these oscillations also exist in Figs. 1 and 3, except that they are nearly invisible in those cases because the disorder ε_- and the displacements being larger, “hide” the oscillations.

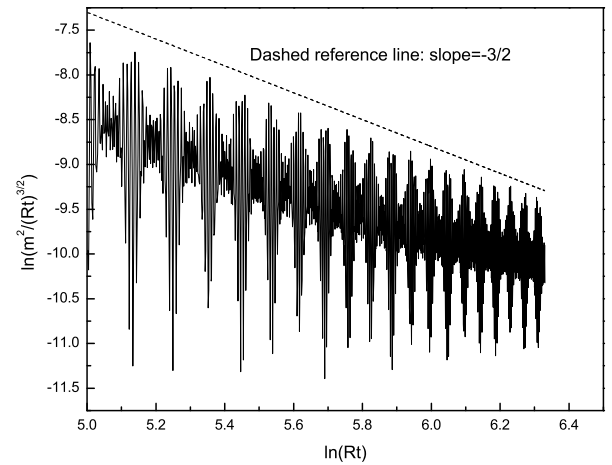


FIG. 2: The mean-square displacement divided by $(Rt)^{3/2}$ for $\beta = edE_1/\omega = 2.405$, $J_0(\beta) = 0$, in the high frequency regime, $R/\omega = 0.3$. The effective hopping constant is $R_{\text{eff}} = 0$, and $\varepsilon_- = |\varepsilon_b - \varepsilon_a| = R/3$. Notice even weak disorder results in bounded displacement, characteristic of localization.

B. Low frequency regime $\frac{R}{\omega} \sim 1$

In Fig. 3 we show the transition from localized to extended state in the low frequency limit. One can see that the transition point is no longer the same as in the high frequency regime $\varepsilon_- = 2R J_0(edE_1/\omega)$. For example, for $\varepsilon_- = R_{\text{eff}} < 2R_{\text{eff}}$ (curve b) the state is sub-diffusive, with $\langle m^2 \rangle \sim t^{0.67}$. As expected, when ε_- is small enough, for example $\varepsilon_- = 0.34R_{\text{eff}}$ (curve a), the state is extended and shows superdiffusive behavior. These results are of course different from the high frequency limits, since in this regime our previous analysis fails. Furthermore, in the extreme low frequency limit, the system tends to that with a DC field: It is known that localized states have a power-law behavior in DC field, instead of the more typical exponential localization in 1D disordered systems.²⁹

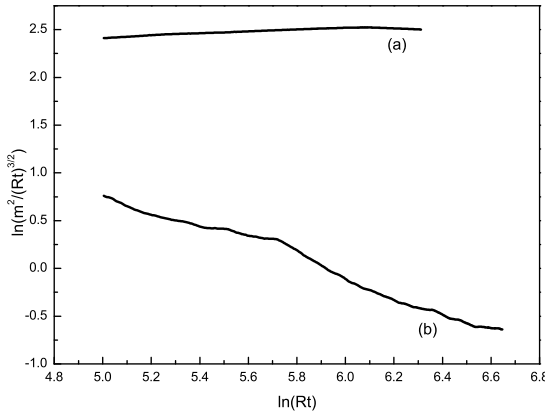


FIG. 3: The mean-square displacement divided by $(Rt)^{3/2}$ for varying amounts of disorder in the low frequency regime $R/\omega = 1$. The amplitude of AC electric field is $edE_1/\omega = 0.7$. The effective hopping constant is $R_{\text{eff}} = 0.8812R$. (a) $\varepsilon_- = 0.34R_{\text{eff}}$ shows extended, superdiffusive behavior; (b) $\varepsilon_- = R_{\text{eff}}$ shows near localization well below the critical value of $\varepsilon_- = 2R_{\text{eff}}$ for high frequency.

C. Inverse participation ratio

To understand more clearly how the AC electric field controls the degree of localization, it is useful to extract information from the Floquet states for the system driven by periodic electric fields. The Floquet states u_m can be expanded with respect to the Wannier states ϕ_l ,

$$u_m(t) = \sum_{l=1}^N c_l^{(m)}(t) \phi_l. \quad (25)$$

We calculate the averaged inverse participation ratio P ,

$$P = \frac{1}{T} \sum_{l=1}^N \int_0^T dt |c_l^{(m)}(t)|^4. \quad (26)$$

If a Floquet state is nearly localized at individual Wannier states, P tends to 1, while P vanishes as $1/N$ if the state is extended; the larger P characterizes a more localized state. In Fig. 4, we show P for different values of $\varepsilon_- = |\varepsilon_b - \varepsilon_a|$ and dimer concentrations versus electric field strength E_1 in the high frequency regime, $R/\omega = 0.1$. We find sharp peaks at $edE_1/\omega = 2.405$, as this value results in $R_{\text{eff}} = 0$, and thus the effective hopping along the chain vanishes. We can enhance the degree of localization in the random dimer model by increasing the detuning ε_- or the dimer concentration Q . For cases (a) and (b) in Fig. 4, Q is the same ($= 0.5$), but ε_- changes from 0.16 in (a) to 0.07 in (b). In contrast, for (b) and (c), the value ε_- is the same, but $Q = 0.2$ is smaller in (c). It is clear that P is larger overall for the more disordered systems, and although a peak appears always at $edE_1/\omega \simeq 2.4$, decreasing disorder suppresses the peak value and overall amplitude of P . One can also

observe that there is a relatively sudden enhancement of P for the system in (a) for $edE_1/\omega \gtrsim 0.9$, while for (b) and (c) this occurs between $edE_1/\omega \simeq 1.7$, and 3.3. From our previous discussion, we know that the localization-delocalization transition occurs at $\varepsilon_- = 2RJ_0(edE_1/\omega)$. From this formula, we find that the transition point for (a) is in fact at $edE_1/\omega = 0.92$, while for (b) and (c) it occurs for $edE_1/\omega = 1.78$, and 3.33. These match very well with our numerical calculation.

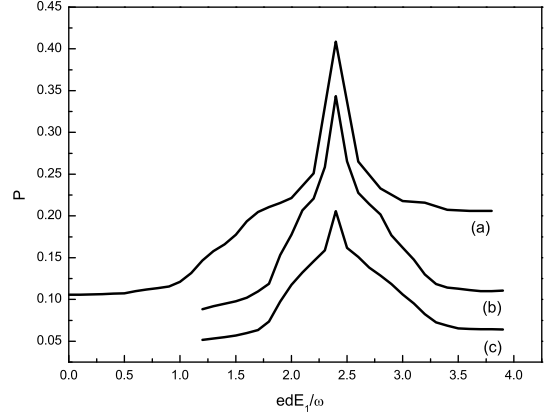


FIG. 4: The averaged inverse participation ratio versus electric fields for the random dimer model. Lattice size $N = 81$ and $R/\omega = 0.1$. (a) $\varepsilon_- = 0.16$, the concentration of dimer of energy ε_b is 50% ($Q = 0.5$); (b) $\varepsilon_- = 0.07$ and $Q = 0.5$; (c) $\varepsilon_- = 0.07$, but with concentration of dimer $Q = 0.2$. Notice localized peak at $edE_1/\omega = 2.4$ has decreasing amplitude with decreasing ε_- or Q . Region of high P values agrees with expected $\varepsilon_- = 2RJ_0(edE_1/\omega)$ (see text).

To elucidate further the role of correlations, we compare P in an Anderson model (without correlations) with a random dimer model system, as shown in Fig. 5. For a more quantitative comparison, we let the variance of the Anderson model distribution, $W^2/12$, be the same as that in the random dimer model, $\frac{1}{2}(\varepsilon_a^2 + \varepsilon_b^2)$. It is evident that P is much larger in the Anderson model (indicating a more localized system), and that P varies smoothly with electric field, indicating no localization-delocalization transition with field.¹² This figure also indicates that an important effect of the presence of the random dimer short range correlations is to delocalize a few states, reducing globally the value of P in the system. It is clear that the dynamical behavior of a system with correlated disorder is a subtle competition between correlation and disorder.

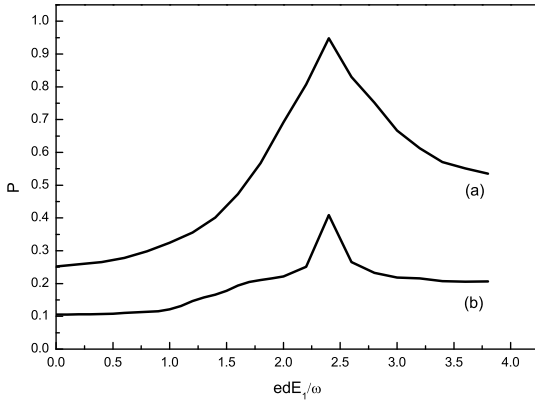


FIG. 5: The averaged inverse participation ratio versus electric fields for random dimer model. Lattice size $N = 81$ and $R/\omega = 0.1$. (a) For Anderson model with $W = \sqrt{6(\varepsilon_a^2 + \varepsilon_b^2)} = 0.392$; (b) for random dimer model with $\varepsilon_b - \varepsilon_a = 0.16$, the concentration of dimer of energy ε_b is 50%. It is clear that the Anderson model with uncorrelated disorder is more localized and has larger P values at all fields.

D. conclusions

We have studied the AC-field controlled random dimer model. The dynamics of our system depends on the

competition between band renormalization (band collapse/dynamic localization), Anderson localization, and the correlation (dimer structure). We find that there is an AC electric field induced transition from extended to localized states, which is absent in the Anderson model. The transition point is found analytically for the high frequency limit, and found to occur when $\varepsilon_- = |\varepsilon_b - \varepsilon_a| \simeq R_{\text{eff}} = 2RJ_0(edE_1/\omega)$. The dynamical localization is not only recovered as a natural limit in the absence of disorder, but also shows its effects in the transport properties of the system with disorder and correlation (the peaks in Figure 4 and 5). The generalization of our results to a N -dimer model is straightforward, and expected to yield qualitatively similar results. Our theoretical predictions could be checked in a variety of systems, and especially on experiments in GaAs-AlGaAs random-dimer superlattices.¹⁵ In experiments, tuning external AC field is a relative easy task compared with changing disorder or correlation in a desired way. Generalizations to different and more complex correlations are also expected to give interesting results.

Acknowledgments

We acknowledge helpful discussions with J. M. Villas-Boas, and support from the US-DOE and the 21st Century Indiana Fund.

¹ E. E. Mendez, F. Agullo-Rueda, and J. M. Hong, Phys. Rev. Lett. **60**, 2426 (1988); E. E. Mendez and G. Bastard, Phys. Today **46**, 34 (1993); C. Martijin de Sterke, J. N. Bright, P. A. Krug, and T. E. Hammon, Phys. Rev. E **57**, 2365 (1998); S. R. Wilkinson, C. F. Bharucha, K. W. Madison, Q. Niu, and M. G. Raizen, Phys. Rev. Lett. **76**, 4512 (1996); M. B. Dahan, E. Peik, J. Reichel, Y. Castin, and C. Salomon, Phys. Rev. Lett. **76**, 4508 (1996).

² R. Tsu and G. H. Dohler, Phys. Rev. B **12**, 680 (1975).

³ X.-G. Zhao, R. Jahnke, and Q. Niu, Phys. Lett. A **202**, 297 (1995).

⁴ K. B. Nordstrom, K. Johnsen, S. J. Allen, A.-P. Jauho, B. Birnir, J. Kono, T. Noda, H. Akiyama, and H. Sakaki, Phys. Rev. Lett. **81**, 457 (1998).

⁵ M. Holthaus and D. W. Hone, Phil. Mag. B **74**, 105 (1996).

⁶ D. H. Dunlap and V. M. Kenkre, Phys. Rev. B. **34**, 3625 (1986); Phys. Lett. A **127**, 438 (1988); X.-G. Zhao, Phys. Lett. A **155**, 299 (1991); **167**, 291 (1992).

⁷ See, for example, M. Grifoni and P. Hänggi, Phys. Rep. **304**, 229 (1998).

⁸ J.M. Villas-Boas, W. Zhang, S.E. Ulloa, P.H. Rivera, and N. Studart, Phys. Rev. B **66**, 085325 (2002).

⁹ J.M. Villas-Boas, S.E. Ulloa, and N. Studart, Phys. Rev. B **70**, 041302 (2004).

¹⁰ D. W. Hone and M. Holthaus, Phys. Rev. B **48**, 15123 (1993).

¹¹ A.-Z. Zhang, P. Zhang, S.-Q. Duan, X.-G. Zhao, and J.-Q. Liang, Phys. Rev. B. **63**, 045319 (2001).

¹² M. Holthaus, G. H. Ristow, and D. W. Hone, Phys. Rev. Lett. **75**, 3914 (1995).

¹³ E. Abrahams, P. W. Anderson, D. C. Licciardello, and T. V. Ramakrishnan, Phys. Rev. Lett. **42**, 673 (1979).

¹⁴ D. H. Dunlap, H.-L. Wu, and P. W. Phillips, Phys. Rev. Lett. **65**, 88 (1990); P. Phillips and H.-L. Wu, Science **253**, 1805 (1991).

¹⁵ V. Bellani, E. Diez, R. Hey, L. Toni, L. Tarricone, G. B. Parravicini, F. Dominguez-Adame, and R. Gomez-Alcalá Phys. Rev. Lett. **82**, 2159 (1999); V. Bellani, E. Diez, A. Parisini, L. Tarricone, R. Hey, G. B. Parravicini, and F. Dominguez-Adame, Physica E **7**, 823 (2000).

¹⁶ J. C. Flores and M. Hilke, J. Phys. A: Math. Gen. **26**, L1255 (1993); A. Bovier, J. Phys. A: Math. Gen. **25**, 1021 (1992).

¹⁷ J. C. Flores, J. Phys. : Condens. Matter **1**, 8471 (1989).

¹⁸ F. Dominguez-Adame, A. Sanchez, and E. Diez, J. Appl. Phys. **81**, 777 (1997).

¹⁹ F. Moura and M. Lyra, Phys. Rev. Lett. **81**, 3735 (1998); *ibid* **84**, 199 (2000).

²⁰ F. M. Izrailev and A. A. Krokhin, Phys. Rev. Lett. **82**, 4062 (1999).

²¹ F. M. Izrailev, A. A. Krokhin, and S. E. Ulloa, Phys. Rev. B **63**, 041102(R) (2001).

²² W. Zhang and S. E. Ulloa, Phys. Rev. B **69**, 153203 (2004), and in preparation.

²³ D. K. Klotsa, R. A. Römer, and M. S. Turner, Biophys. J. **89**, 2187 (2005), and cond-mat/0508720.

²⁴ exciton hopping by Dominguez-Adame in PRL ...

²⁵ *Handbook of Mathematical Functions*, M. Abramowitz and I. A. Stegun, eds. (Dover, New York, 1965).

²⁶ E. H. Cannon, K. N. Alekseev, F. V. Kusmartsev, and D. K. Campbell, Europhysics Lett. **56**, 842 (2001).

²⁷ S. N. Evangelou and A. Z. Wang, Phys. Rev. B **47**, 13126 (1993).

²⁸ M. Holthaus, Phys. Rev. Lett. **69**, 351 (1992); W. Zhang and X.-G. Zhao, Physica E **9**, 667 (2001).

²⁹ C. M. Soukoulis, J. V. Jose, E. N. Economou, and P. Sheng, Phys. Rev. Lett. **50**, 754 (1983); F. Delyon, B. Simon, and B. Souillard, Phys. Rev. Lett. **52**, 2187 (1984).